

# A comparison between the vacuum ultraviolet photoionization time-of-flight mass spectra and the GC/MS total ion chromatograms of polycyclic aromatic hydrocarbons contained in coal soot and multi-component PAH particles

Shaokai Gao, Yang Zhang, Yao Li, Junwang Meng, Hong He, Jinian Shu\*

Research Center for Eco-Environmental Sciences, Chinese Academy of Sciences, 18 Shuangqing Road, Haidian District, Beijing 100085, China

## ARTICLE INFO

### Article history:

Received 24 January 2008

Received in revised form 5 May 2008

Accepted 5 May 2008

Available online 9 May 2008

### Keywords:

Aerosol mass spectrometer

PAHs

Vacuum ultraviolet photoionization

Mass spectrum

Soot

## ABSTRACT

This paper reports a comparison between the vacuum ultraviolet photoionization time-of-flight mass spectra and the gas chromatography–mass spectrometry total ion chromatograms of polycyclic aromatic hydrocarbons (PAHs) contained in soot particles and multi-component PAH particles. The soot particles are produced by burning a small amount of screened bituminous coal powder in a tubular oven under synthesized air. The soot particles generated are analyzed on-line with a vacuum ultraviolet photoionization aerosol time-of-flight mass spectrometer (VUV-AMS) and off-line with a gas chromatography–mass spectrometer (GC/MS). 55 PAHs are observed with the GC/MS, while parent ions of 54 PAHs are observed with the VUV-AMS. The multi-component PAH particles are generated by atomizing 16 PAHs in isopropyl alcohol. The PAHs are defined as 16 primary pollutants by the Environmental Protection Agency of the United States. GC/MS identifies the 16 PAHs while VUV-AMS observes 15 PAHs with missing the mass peak of naphthalene. The relationship of the PAH sensitivity of VUV-AMS and GC/MS vs. the molecular weights of the PAHs are obtained.

© 2008 Elsevier B.V. All rights reserved.

## 1. Introduction

Ambient organic aerosols often contain hundreds of organic components, such as alkanes, hopanes, steranes, alkanoids, aromatic acids, polycyclic aromatic hydrocarbons (PAHs), alkanols, humic acids, etc. [1,2]. The most knowledge about the composition of organic aerosols today is obtained by gas chromatography–mass spectrometry (GC/MS) [3]. Coupled with a mass spectrometer, GC is a wonderful instrument which can analyze most of the volatile and semi-volatile organics with both quantification and species identification. A typical mass spectrometer combined with GC is a quadrupole mass spectrometer with electron impact ionization. It is well known that every organic chemical has a specific daughter ion pattern when it is ionized by 70 eV electron impact (EI). Therefore, after separating the sample according to different retention times of various compounds on the GC columns, GC/MS discriminates each compound by matching the daughter ion patterns resulted from the EI ionization with the standard database. Although the GC/MS method has exhibited a high selectivity and sensitivity in analyzing the trace level of organic pollutants in air [4], soil and water [5], it cannot present real-time analysis. Moreover, it

has the drawback of time consuming and labor intensive and man made errors are often introduced during the sample pretreatment processes.

The aerosol mass spectrometers (AMSs) have been developed and improved to fulfill the need to analyze aerosol particles on-line and in real-time since 1990 [6]. Briefly, the AMS analyzes particles by vaporizing the particles, ionizing nascent vapor and then detecting the ions. Different combinations of vaporization, ionization and detection techniques make different types of the AMS. Thermal vaporization/electron impact/quadrupole mass filter and single laser desorption/ionization/reflectron mass spectrometer are the combinations used mostly by AMS. They all can achieve analyzing some kind of particles in real-time. Recently, many efforts have been made to analyze organic aerosols by combining the VUV photoionization technique with the aerosol mass spectrometer [7–14]. Compared to the widely used ionization methods such as EI or UV laser ablation, VUV photoionization is relatively soft, thus organic molecules can be ionized without intensive dissociation and the parent ion peaks of most organic molecules can be observed. Therefore, this method offers a possibility to quantify and identify components of ambient organic aerosols in real-time.

Until now, several papers have focused on the detection of PAHs in smoke or soot originating from all kinds of sources such as cigarettes [15,16], woods [17] and diesel engines [18,19]. In the

\* Corresponding author. Tel.: +86 10 62849508; fax: +86 10 62923563.  
E-mail address: [jshu@rcees.ac.cn](mailto:jshu@rcees.ac.cn) (J. Shu).

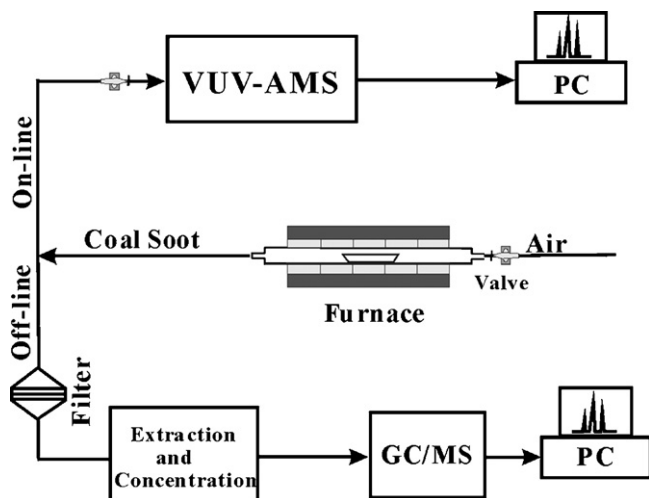


Fig. 1. Schematic diagram of the experimental setup.

present work, coal soot and a standard mixture of 16 U.S. EPA-regulated PAHs are analyzed both on-line with a vacuum ultraviolet photoionization aerosol time-of-flight mass spectrometer (VUV-AMS) and off-line with a gas chromatography–mass spectrometer (GC/MS). 54 PAHs in the coal soot particles observed with the VUV-AMS are identified with the GC/MS. The VUV-AMS results of the standard mixture of 16 U.S. EPA-regulated PAHs show that only naphthalene is missed in the vacuum ultraviolet photoionization time-of-flight mass spectrum. Detailed results are described in following sections.

## 2. Experimental

The schematic diagram of the experimental setup is shown in Fig. 1. The main analytical instruments used in the experiment are a VUV-AMS and a GC/MS. The VUV-AMS is newly home-built. The detailed description about the design of the VUV-AMS is presented elsewhere [20]. So only a brief description is offered here. A nozzle of  $\sim 0.12$  mm orifice combined with an aerodynamic lens assembly and a three stage differential pumping system is used to sample particles directly at atmospheric pressure. The sample flow rate is  $\sim 1.3$  cm<sup>3</sup> atm s<sup>-1</sup>. The three stage differential pumping system is composed of a source chamber, a differential chamber, and a detection chamber. A heater tip used to vaporize organic particles is placed in the detection chamber. The heater tip (up to 600 K) is an 8-mm diameter copper rod coupled to a cartridge heater driven by a dc power supply. The vapor generated from particles is photoionized with light radiated from a RF-powered VUV lamp. The photon energy of the main output is 10 eV (123.6 nm, Kr atom resonance line). The total photon flux output from the VUV lamp is about  $2 \times 10^{12}$  photon/s. The ions produced by VUV photoionization are detected with a reflectron mass spectrometer. The reflectron mass spectrometer is characterized with a field-free flight distance of 1.4 m, an ion mirror and a chevron multichannel plate detector. The GC/MS is a commercial instrument purchased from Agilent Technologies, which is characterized with a Hewlett-Packard (HP) 6890 gas chromatography equipped with a 30 m  $\times$  0.25 mm  $\times$  0.25  $\mu$ m HP-5 capillary and a HP-5973 quadrupole mass filter with a 70 eV electron impact ionizer.

The soot particles used in the experiment are prepared by combusting  $\sim 10$  g 75-mesh Inner Mongolia bituminous coal in a tubular oven. The working temperature of the tubular oven is set at 873 K for the comparison experiment. The soot particles produced by combustion are flushed out with 1.5 l/min synthetic air controlled by

a ball-float flowmeter. After passing a 2.5-m long conductive rubber tube, the soot particles are continuously sampled and analyzed with the VUV-AMS. The combustion of  $\sim 10$  g coal powder under the experimental condition usually takes 5–6 min to complete. Mass spectra are recorded from the beginning to the end of the coal combustion process. Each mass spectrum is collected in 30 s and it takes  $\sim 5$  s to save files on average. Generally, 10 files are recorded for a whole combustion process.

For off-line analysis, the soot particles entrained in the  $\sim 1.5$  l/min flow are collected on an organically clean glass fiber filter ( $\Phi 25$ , annealed at 723 K for 4 h)  $\sim 1.5$  m downstream of the tubular oven. Sampling begins when coal powder is fed in and stops when soot smoke disappears. The process usually takes 5–6 min. After sampling, the filters are taken out and placed in clean 200 ml jars with Teflon lined lids filled with 60 ml dichloromethane (DCM). The filters are all extracted ultrasonically three times, respectively. Each extraction lasts 30 min. The extracts are mixed together, filtered and concentrated with a rotary evaporator (bath temperature  $\leq 313$  K). Interfering compounds are removed by liquid–solid chromatography using a silica column (the silica gel is preheated at 423 K for 12 h). The PAH fraction is eluted out by a mixture of DCM and hexane (1:1, v/v). Then it is concentrated with a rotary evaporator again and is further reduced to  $\sim 0.5$  ml by blowing with a gentle stream of nitrogen. The chromatographic conditions are as follows: injector temperature, 553 K; ion source temperature, 453 K; temperature program: 338 K (5 min), 338–563 K at 5 K/min, 563 K (20 min). The carrier gas is helium at a constant flow rate of 1.5 ml/min. The sample of 1  $\mu$ l is injected with the splitless model. The mass range from 50 to 510 Da is used for qualitative determination. Data acquisition and processing are controlled by a HP Chemstation data system. PAHs that have the corresponding standard compounds are identified by the retention time while others are distinguished by matching the daughter ion patterns with the standard database (matching degree  $>85\%$ ).

Known components of PAH aerosol particles are generated by atomizing 1 ml standard mixture (methanol:methylene chloride = 1:1) of 16 U.S. EPA-regulated PAHs (used for GC/MS calibration) in 9 ml isopropyl alcohol. The gas flow for the atomization is controlled by a ball-float flowmeter. A  $\sim 1.5$  l/min flow rate is maintained in the experiment. The liquid consumption rate of isopropyl alcohol in the experiment is  $\sim 0.33$  ml/min. The mass concentration of the aerosols produced can be calculated with the formula  $c \times r/f$  ( $c$ : concentration of the solution;  $r$ : liquid consumption rate;  $f$ : flow rate of gas).

All reagents are of chromatographic grade, from J.T. Baker Co. The standard mixture of 16 U.S. EPA-regulated PAHs is ordered from Sigma–Aldrich. The anhydrous sodium sulfate (analytical grade) and the silica gel (chromatographic grade 100–200 mesh) are purchased from Qingdao Chemical plant in China. The Inner Mongolia bituminous coal is purchased from a coal storage and transportation station in Beijing.

## 3. Results and discussion

Fig. 2 shows four VUV photoionization time-of-flight mass spectra of the soot particles with the heater temperatures at 333, 393, 423, and 483 K. The fresh soot sample is prepared for each heater temperature by putting  $\sim 10$  g coal powder in the tubular oven, which is operated at 873 K. The data acquisition of the mass spectrum starts at the beginning of the combustion of the coal powder. Each mass spectrum is collected in 30 s and normalized by the peak intensity at  $m/z$  178. There is a few seconds deviation between the start time of the collection of each mass spectrum due to manual synchronization, which slightly affects the intensities of the

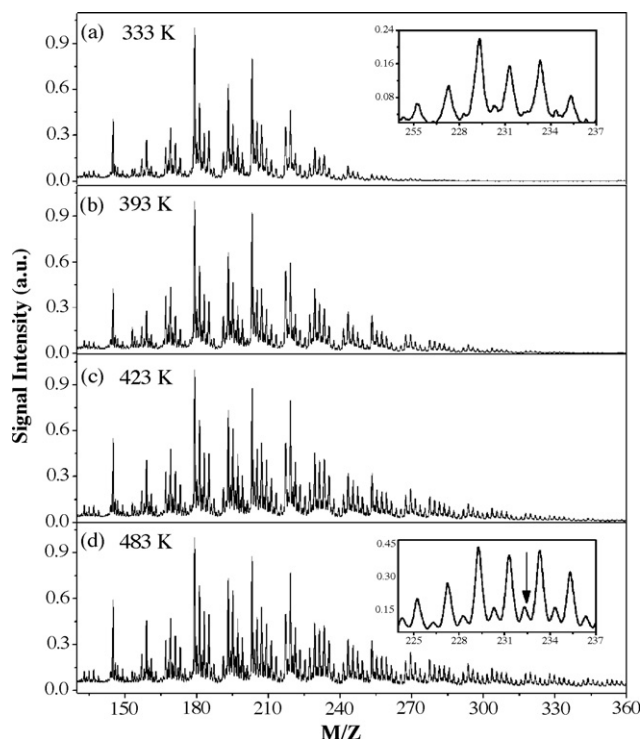


**Fig. 2.** VUV photoionization time-of-flight mass spectra of the coal soot with the heater temperature at (a) 333 K, (b) 393 K, (c) 423 K and (d) 483 K. Each mass spectrum is collected in 30 s and normalized by the peak intensity at  $m/z$  178.

mass peaks. New heavier mass ions (above 250  $m/z$ ) continuously appear when the heater temperature is increased from 333 to 483 K indicating a better vaporization efficiency of the compounds at the higher heater temperature. Generally, vaporization and ionization of the thermally labile species are often accompanied with possible chemical bond cleavage (fragmentation) due to the internal energy imparted to the organic molecular by the heater or the ionization source [21]. Compared with the zoomed plot in Fig. 2(a), the minor peaks indicated with an arrow sign in the zoomed plot in Fig. 2(d) become more intensive as the heater temperature rises, which reveals that severer fragmentation of molecules occurs. Concerning of the potential fragmentation of molecules induced by heating, 393 K is chosen as the heater temperature for the comparison experiment.

The temperature of the tubular oven is critical to the composition of soot contents. Fig. 3(a), (b), (c) and (d) shows the VUV photoionization time-of-flight mass spectra of soot particles generated from the tubular oven at 673, 873, 1073 and 1273 K, respectively. The heater temperature is 393 K as stated above. The data acquisition of the mass spectrum starts at the beginning of the combustion of the coal powder. Each mass spectrum is collected in 30 s and normalized with the peak intensity of its strongest peak. The most intense peak in Fig. 3(a) is assigned to the parent ion of  $C_4$ -alkylated phenanthrene (3,4,5,6-tetramethylphenanthrene), which is the most abundant organic chemical contained in the coal sample and is identified with the GC/MS analysis of the coal extract. This is in consistent with the results from Cao et al. and Bente et al. [22,23]. Their results showed an abnormally abundant mass peak representing alkylated phenanthrene during combustion. The GC/MS analysis shows that most of the mass peaks shown in Fig. 3(a) and (b) are from homologue rows of PAHs as well as its alkylated derivatives and furans. When the temperature of the tubular oven rises above 1273 K (Fig. 3(d)), only the most stable compounds survive and the derivatives of PAHs (alkylated PAHs or

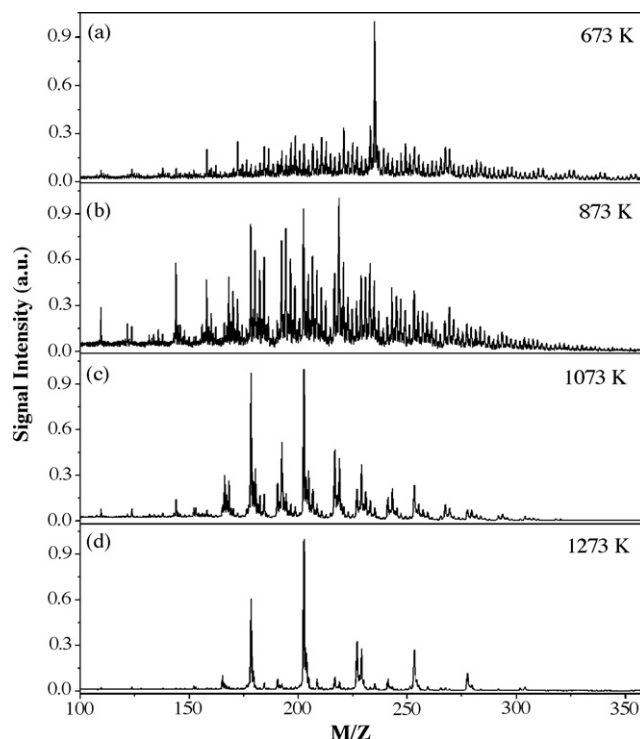


**Fig. 3.** VUV photoionization time-of-flight mass spectra of the coal soot produced with the oven temperature at (a) 673 K, (b) 873 K, (c) 1073 K and (d) 1273 K. Each mass spectrum is collected in 30 s and normalized with the peak intensity of its strongest peak.

furans) reduce to their skeletal structures without side chains. Both Fig. 3(c) and (d) show that PAHs with less degree of alkylation prevail, which indicates a more complete combustion process at high temperatures [23]. Fig. 3(b) shows that the soot particles generated in the 873 K tubular oven contain relatively more abundant and complex organic chemicals. Therefore, 873 K is chosen as the temperature of the oven for the comparison experiment.

Fig. 4 shows VUV photoionization time-of-flight mass spectrum (a) and the GC/MS total ion chromatogram (b) of soot particles. The mass spectrum shown in Fig. 4(a) is obtained by accumulating all the mass spectra, each of which is respectively collected in 30 s from the beginning to the end of combustion of a ~10 g coal sample. The mass spectrum and GC/MS total ion chromatogram are normalized with the intensity of their strongest peaks, respectively. Table 1 lists the peak intensities of PAHs observed in Fig. 4(a) and (b). The dotted line in Fig. 4(a) is the peak intensities of PAHs obtained with GC/MS plotted vs.  $m/z$ . The most intense peak in both the mass spectrum and total ion chromatogram is at 202  $m/z$  (pyrene). The relative intensities of other PAH mass peaks measured with the VUV-AMS are higher than those measured with the GC/MS except for the peaks at 212, 234 and 242  $m/z$ , which, respectively represents 2,6-diisopropyl-naphthalene, 3,4,5,6-tetramethylphenanthrene and single methylated chrysene. The following three reasons may result in the discrepancies between the measurements with the VUV-AMS and GC/MS: (1) the different ionization methods used by the GC/MS and VUV-AMS, (2) the different extraction efficiencies for various organic compounds and the chemical degradation of the PAHs on the filters, (3) the possible contributions from the non-PAH molecules to the peak intensities of the mass spectrum by its own or its fragments. Some mass peaks in Fig. 4(a) which are not listed in Table 1 may suggest the presence of highly reactive PAHs such as cyclopenta[cd]pyrene ( $m/z$  = 226). These chemicals could be sampled and observed by the VUV-AMS but degraded

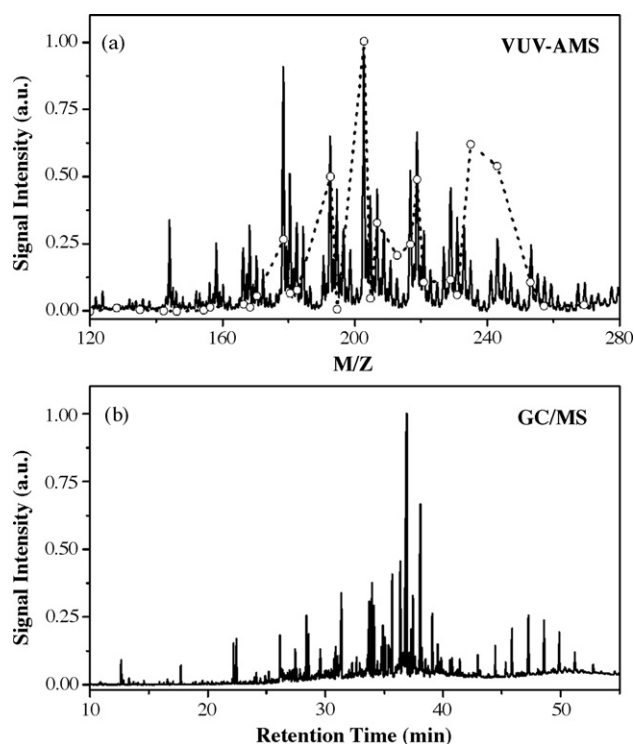


**Fig. 4.** (a) VUV photoionization time-of-flight mass spectrum of the coal soot produced with the oven temperature at 873 K and the heater temperature at 393 K. The mass spectrum is obtained by accumulating all the VUV-TOF mass spectra, each of which is collected in 30 s from the beginning to the end of combustion of a  $\sim 10$  g coal sample. (b) GC/MS total ion chromatogram of the coal soot extract.

on the filter sampler, and thus missed in the GC/MS total ion chromatogram.

Fig. 5 shows the VUV photoionization time-of-flight mass spectrum (a) and GC/MS total ion chromatogram (b) of the standard mixture of 16 U.S. EPA-regulated PAHs. Table 2 lists the PAH concentration of the standard mixture and the fractional mass concentration of the PAH particles. The mass spectrum is collected in 100 s. The minor mass peaks at 44, 45, 49, and 60  $m/z$  in Fig. 5(a) are speculated from solvent chemicals. The mass peaks at 44, 45, and 60 can be assigned to  $C_2H_4O^+$ ,  $C_2H_5O^+$ , and  $C_3H_8O^+$ , which are resulted from isopropyl alcohol molecules and its fragments. The mass peak at 49  $m/z$  might be assigned to  $CH_2^{35}Cl^+$ . There is a very small bump at 51  $m/z$ , which might be resulted from  $CH_2^{37}Cl^+$ . The mass peaks at 152, 154, 166, and 278  $m/z$  in Fig. 5(a) are assigned to  $C_{12}H_8^+$  (acenaphthylene ion),  $C_{12}H_{10}^+$  (acenaphthene),  $C_{13}H_{10}^+$  (fluorene), and  $C_{22}H_{14}^+$  (dibenz(*a,h*)anthracene), respectively. Since isomers have the same molecular weight, they cannot be distinguished by the VUV-AMS. The mass peaks at 178, 202, 228, and 276  $m/z$  in Fig. 5(a) are assigned to  $C_{14}H_{10}^+$  (phenanthrene and anthracene),  $C_{16}H_{10}^+$  (fluoranthene and pyrene),  $C_{18}H_{12}^+$  (benzo(*a*)anthracene and chrysene), and  $C_{22}H_{12}^+$  (benzo(*g,h,i*)perylene and indeno(1,2,3-*cd*)pyrene). The mass peak at 252  $m/z$  is contributed from the benzo(*a*)pyrene, benzo(*b*)fluoranthene, and benzo(*k*)fluoranthene ions. Table 2 lists the assignments for the mass peaks in Fig. 5. The intensities of the VUV-AMS and GC/MS signals listed in Table 2 are obtained by integrating their respective peak area and normalizing with the corresponding PAH concentration and the maximum peak area, the GC/MS identifies the 16 PAHs while VUV-AMS observes 15 PAHs with missing the mass peak of naphthalene. No fragment ions of the PAHs are observed in Fig. 5(a). The lower peaks on right side of PAH peaks are the isotope-shift peaks resulted from  $^{13}C$ . The PAH molecules are usually resistant to fragmentation during ionization processes due to the stabilizing effect of their delocalized

**Table 1**  
Peak intensities of PAHs contained in coal soot measured with the GC/MS and VUV-AMS

PAH name	Formula	MW	GC/MS	AMS
Benzene, trimethyl-	$C_9H_{12}$	120	0.0035	0
Naphthalene	$C_{10}H_8$	128	0.015	0.051
Benzothiazole	$C_7H_5SN$	135	0.0091	0.073
Naphthalene, monomethyl-	$C_{11}H_{10}$	142	0.0057	0.37
Benzene, 1,4-dichloro-	$C_6H_4Cl_2$	146	0.003	0.08
Biphenyl	$C_{12}H_{10}$	154	0.0075	0.13
Naphthalene, dimethyl-	$C_{12}H_{12}$	156	0.018	0.28
Fluorene	$C_{13}H_{14}$	166	0.029	0.26
Diphenylmethane/biphenyl, monomethyl-/dibenzofuran	$C_{13}H_{12}$	168	0.018	0.35
Naphthalene, trimethyl-	$C_{13}H_{14}$	170	0.06	0.23
Anthracene/phenanthrene	$C_{14}H_{10}$	178	0.27	0.93
9H-Fluorene, monomethyl-	$C_{14}H_{12}$	180	0.07	0.54
Dibenzofuran, monomethyl-/4,4'-dimethylbiphenyl-[1,1'-Biphenyl]-4-carboaldehyde/2-hydroxyfluorene	$C_{13}H_{10}O$	182	0.081	0.36
Anthracene/phenanthrene, monomethyl-	$C_{15}H_{12}$	192	0.5	0.68
9H-Fluorene, dimethyl-	$C_{15}H_{14}$	194	0.011	0.48
Pyrene	$C_{16}H_{10}$	202	1	1
Naphthalene, 2-phenyl-	$C_{16}H_{12}$	204	0.051	0.46
Phenanthrene, monoethyl-/dimethyl-	$C_{16}H_{14}$	206	0.33	0.48
2,6-Diisopropyl-naphthalene	$C_{16}H_{20}$	212	0.21	0.15
Fluoranthene, monomethyl-/pyrene, monomethyl-	$C_{17}H_{12}$	216	0.25	0.55
Benzo[ <i>k,l</i> ]xanthene	$C_{16}H_{10}O$	218	0.49	0.69
Butylated, hydroxytoluene	$C_{15}H_{24}O$	220	0.11	0.33
Triphenylene/benzo[ <i>a</i> ]anthracene	$C_{18}H_{12}$	228	0.12	0.48
Pyrene, dimethyl-	$C_{18}H_{14}$	230	0.065	0.38
Phenanthrene, tetramethyl-	$C_{18}H_{18}$	234	0.62	0.22
Chrysene, monomethyl-	$C_{19}H_{14}$	242	0.54	0.3
Benzo[ <i>a</i> ]pyrene/benzo[ <i>e</i> ]pyrene	$C_{20}H_{12}$	252	0.11	0.27
Benzo[ <i>c</i> ]phenanthrene, 5,8-dimethyl-	$C_{20}H_{16}$	256	0.022	0.15
Dinaphtho[1,2- <i>b</i> :1'2'- <i>d</i> ]furan	$C_{20}H_{12}O$	268	0.027	0.13

The GC/MS or AMS signal intensity is equal to their respective peak area normalized with the value of the most intensive peak. Isomers or compounds that have the same molecular weight are summarized into one group.

**Table 2**  
GC/MS and VUV-AMS relative sensitivities for the 16 EPA-regulated PAHs

Name	Formula	MW	C <sup>a</sup>	FC <sup>b</sup>	GC/MS	RT	AMS
Naphthalene	C <sub>10</sub> H <sub>8</sub>	128.17	1052.0	23.14	0.31	13.32	0
Acenaphthylene	C <sub>12</sub> H <sub>8</sub>	152.19	2103.0	46.27	0.39	20.72	0.005
Acenaphthene	C <sub>12</sub> H <sub>10</sub>	154.20	1056.0	23.23	0.40	21.62	0.007
Fluorene	C <sub>13</sub> H <sub>10</sub>	166.22	209.1	4.60	0.84	23.99	0.056
Phenanthrene	C <sub>14</sub> H <sub>10</sub>	178.33	103.7	2.28	0.85	28.55	0.26
Anthracene	C <sub>14</sub> H <sub>10</sub>	178.23	103.4	2.27		28.35	
Fluoranthene	C <sub>16</sub> H <sub>10</sub>	202.25	214.2	4.71	0.77	34.84	0.4
Pyrene	C <sub>16</sub> H <sub>10</sub>	202.25	96.9	2.13		33.89	
Benzo(a)anthracene	C <sub>18</sub> H <sub>12</sub>	228.29	104.4	2.30	0.44	40.57	1
Chrysene	C <sub>18</sub> H <sub>12</sub>	228.29	104.1	2.29		40.74	
Benzo(a)pyrene	C <sub>20</sub> H <sub>12</sub>	252.31	107.0	2.35	0.50	45.4	0.89
Benzo(k)fluoranthene	C <sub>20</sub> H <sub>12</sub>	252.31	104.1	2.29		45.3	
Benzo(b)fluoranthene	C <sub>20</sub> H <sub>12</sub>	252.31	210.0	4.62		46.52	
Benzo(g,h,i)perylene	C <sub>22</sub> H <sub>12</sub>	276.33	206.1	4.53	0.99	51.99	0.71
Indeno(1,2,3-cd)pyrene	C <sub>22</sub> H <sub>12</sub>	276.33	101.8	2.24		50.68	
Dibenzo(a,h)anthracene	C <sub>22</sub> H <sub>14</sub>	278.35	207.0	4.55	1.00	50.88	0.99

RT is the retention time of PAHs, its unit is minute. The GC/MS or AMS signal intensity is equal to their respective peak area normalized with the fractional PAH concentration and the area of the most intense peak.

<sup>a</sup> C stands for the PAH concentration of mixture and its unit is  $\mu\text{g}/\text{ml}$ .

<sup>b</sup> FC is the fractional concentration of PAHs in the particle phase, its unit is  $\text{mg}/\text{m}^3$ .

$\pi$ -electrons. The parent ions of the PAH molecules can be observed even with harder ionization techniques, such as EI [24]. Therefore, the method of soft VUV photoionization and the non-branched PAH samples used may mainly account for the complete fragment-free character for the PAHs shown in Fig. 5(a).

Fig. 6 shows the relative sensitivity of the VUV-AMS and GC/MS vs. the molecular weights of PAHs. The line with triangles represents the sensitivity of the VUV-AMS while the line with open circles stands for the sensitivity of the GC/MS. The sensitivity of GC/MS to the 16 PAHs is relatively uniform. The PAHs sensitivity curve of the VUV-AMS first increases monotonically with the molecular weight (2–4 aromatic rings) and reaches a maximum

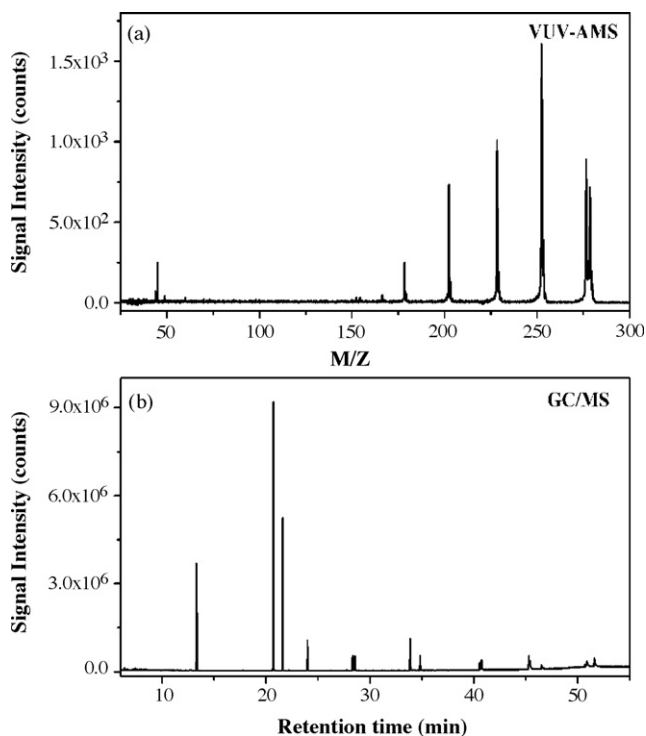


**Fig. 5.** (a) VUV photoionization time-of-flight mass spectrum of the standard mixture of 16 U.S. EPA-regulated PAHs, (b) GC/MS total ion chromatogram of the standard mixture of 16 U.S. EPA-regulated PAHs. The mass spectrum is collected in 100 s.

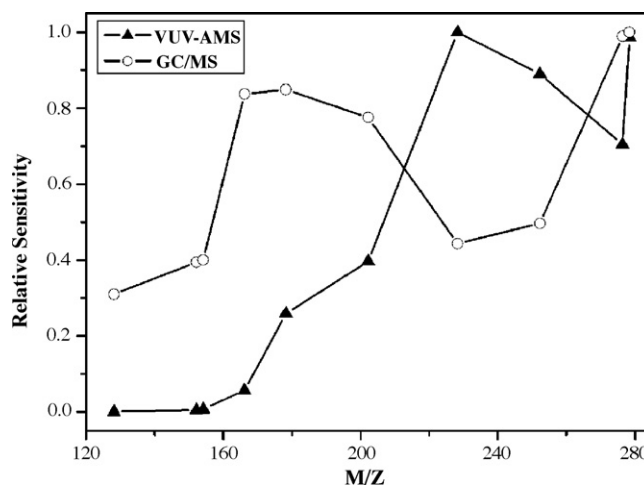


**Fig. 6.** VUV-AMS and GC/MS relative sensitivity for 16 U.S. EPA-regulated PAHs. The line with triangles represents the sensitivity of the VUV-AMS while the line with open circles stands for the sensitivity of the GC/MS.

point at 202 amu. Then the curve falls  $\sim 30\%$  at 252 amu and reaches another maximum point at 278 amu. We think that the PAH sensitivity curve of the VUV-AMS shown in Fig. 6 partly reflects the photoionization efficiencies of these PAHs ionized with this VUV lamp. Besides, a portion of the lighter PAHs contained in the particles may be lost to the gas phase during transportation from the atomizer to the VUV-AMS.

#### 4. Conclusion

This paper reports a comparison between the vacuum ultraviolet photoionization time-of-flight mass spectra and the gas chromatography–mass spectrometry total ion chromatograms of polycyclic aromatic hydrocarbons contained in soot and multi-component PAH particles. The experimental results show that the measurements with the GC/MS and VUV-AMS are pretty consistent in identifying species of PAHs. However, there is a large discrepancy in the relative signal intensity of the single PAH molecule between these two methods. Quantification remains to be a challenge to the VUV-AMS due to the large difference of photoionization efficiency between the PAH molecules and the possible overlaps of

the non-PAH molecules' fragments to the mass peaks of PAHs. The fragment-free mass spectrum of 16 U.S. EPA-regulated PAHs except naphthalene can be obtained with this VUV-AMS. The GC/MS has the relatively uniform sensitivity to PAHs while the VUV-AMS is more sensitive to the larger PAHs (more than three rings) among the 16 U.S. EPA-regulated PAHs.

### Acknowledgements

This research was supported by the funding for creative research groups of China (Grant No. 50621804) and the funding from National Natural Science Foundation of China (Grant No. 20673138). The authors would like to thank Dr. Shaoyong Huang for his help during the GC/MS experiment.

### References

- [1] J.J. Schauer, W.F. Rogge, L.M. Hildemann, M.A. Mazurek, G.R. Cass, *Atmos. Environ.* 30 (1996) 3837.
- [2] E. Schnelle-Kreis, M. Sklorz, A. Peters, J. Cyrys, R. Zimmermann, *Atmos. Environ.* 39 (2005) 7702.
- [3] D.L. Poster, M.M. Schantz, L.C. Sander, S.A. Wise, *Anal. Bioanal. Chem.* 386 (2006) 859.
- [4] A.H. Falkovich, Y. Rudich, *Environ. Sci. Technol.* 35 (2001) 2326.
- [5] F. Hernandez, J. Beltran, F.J. Lopez, J.V. Gaspar, *Anal. Chem.* 72 (2000) 2313.
- [6] C.A. Noble, K.A. Prather, *Mass Spectrom. Rev.* 19 (2000) 248.
- [7] M.R. Canagaratna, J.T. Jayne, J.L. Jimenez, J.D. Allan, M.R. Alfarra, Q. Zhang, T.B. Onasch, F. Drewnick, H. Coe, A. Middlebrook, A. Delia, L.R. Williams, A.M. Trimborn, M.J. Northway, P.F. DeCarlo, C.E. Kolb, P. Davidovits, D.R. Worsnop, *Mass Spectrom. Rev.* 26 (2007) 185.
- [8] E. Gloaguen, E.R. Mysak, S.R. Leone, M. Ahmed, K.R. Wilson, *Int. J. Mass Spectrom.* 258 (2006) 74.
- [9] E.R. Mysak, K.R. Wilson, M. Jimenez-Cruz, M. Ahmed, T. Baer, *Anal. Chem.* 77 (2005) 5953.
- [10] M.J. Northway, J.T. Jayne, D.W. Toohey, M.R. Canagaratna, A. Trimborn, K.I. Akiyama, A. Shimono, J.L. Jimenez, P.F. DeCarlo, K.R. Wilson, D.R. Worsnop, *Aerosol Sci. Technol.* 41 (2007) 828.
- [11] B. Oktem, M.P. Tolocka, M.V. Johnston, *Anal. Chem.* 76 (2004) 253.
- [12] T. Streibel, S. Mitschke, T. Adam, J. Weh, R.J. Zimmermann, *Anal. Appl. Pyrol.* 79 (2007) 24.
- [13] D.C. Sykes, E. Woods, G.D. Smith, T. Baer, R.E. Miller, *Anal. Chem.* 74 (2002) 2048.
- [14] E. Woods, G.D. Smith, Y. Dessiaterik, T. Baer, R.E. Miller, *Anal. Chem.* 73 (2001) 2317.
- [15] T. Adam, S. Mitschke, T. Streibel, R.R. Baker, R. Zimmermann, *Anal. Chim. Acta* 572 (2006) 219.
- [16] R. Zimmermann, H.J. Heger, A. Kettrup, *Fresenius J. Anal. Chem.* 363 (1999) 720.
- [17] T.E. Hauler, U. Boesl, S. Kaesdorf, R.J. Zimmermann, *Chromatogr. A* 1058 (2004) 39.
- [18] L. Oudejans, A. Touati, B.K. Gullett, *Anal. Chem.* 76 (2004) 2517.
- [19] S.M. Toner, D.A. Sodeman, K.A. Prather, *Environ. Sci. Technol.* 40 (2006) 3912.
- [20] J.N. Shu, S.K. Gao, Y. Li, *Aerosol Sci. Technol.* 42 (2008) 110.
- [21] K.R. Wilson, M. Jimenez-Cruz, C. Nicolas, L. Belau, S.R. Leone, M.J. Ahmed, *Phys. Chem. A* 110 (2006) 2106.
- [22] M. Bente, T. Adam, T. Ferge, S. Gallavardin, M. Sklorz, T. Streibel, R. Zimmermann, *Int. J. Mass Spectrom.* 258 (2006) 86.
- [23] L. Cao, F. Muhlberger, T. Adam, T. Streibel, H.Z. Wang, A. Kettrup, R. Zimmermann, *Anal. Chem.* 75 (2003) 5639.
- [24] K. Dzepina, J. Arey, L.C. Marr, D.R. Worsnop, D. Salcedo, Q. Zhang, T.B. Onasch, L.T. Molina, M.J. Molina, J.L. Jimenez, *Int. J. Mass Spectrom.* 263 (2007) 152.